Rainsplash Erosion for Natural Slopes and Rainfall Conditions

Bettina Martínez-Hackert [a], Marcus I. Bursik [b]

[a] *Dept. of Earth Sciences and Science Education, Buffalo State College, 1300 Elmwood Avenue, Buffalo, NY 14222*

[b] *Dept. of Geology, State University of New York at Buffalo, 411 Cooke Hall, Buffalo, NY 14260* *(mib@buffalo.edu)*

Abstract

Rainsplash is significant for interrill erosion since it facilitates the movement of loosened soil frangments. Because it is a technically difficult process to measure, many studies focus on experimental simulation under controlled conditions both in field and laboratory. Raindrop erosion studies have produced models to predict the erosivity due to raindrop impact on varying ground surfaces, with a focus on agricultural soils and generally low slope gradients.

This study focuses on rainsplash measurements under natural slope and rainfall conditions. We recorded natural precipitation, local slope angle, vegetation cover locally modified by wildland fire, and soil bulk density for areas where rainsplash was collected on two scoria cones in the San Francisco Volcanic Field, AZ. Samples were collected using splashboards, hence allowing the measurement of netdownslope sediment yield by collecting upslope splashed and downslope splashed sediment. Results of this study indicate a large amount of slope material being moved in the first rainfall events of the season with increased erosion rates in areas affected by wildland

fire. Using multiple regresssion we are able to distinguish between three different types of fire severity populations.

Key words:

Rainsplash, Raindrop erosion, Hillslope erosion, Diffusion type erosion, Natural rainfall conditions, Natural slope conditions, Steep slope, San Francisco Volcanic Field, Semiarid climate, Arizona, rain erosion

---

1 Introduction

Most studies of raindrop impact erosion have measured the raindrop energy necessary to detach and disaggregate soil particles (Torri and Poesen, 1992; Wainwright et al., 1999; Salles and Poesen, 2000; Pietraville et al., 2001; Van Dijk et al., 2003a). Erosion by rainsplash increases exponentially with rainfall intensity until ponding is achieved, then rainsplash erosion decreases as overland flow sets in (Ellison, 1944; Schultz et al., 1985; Wainwright et al., 1995; Mouzai and Bouhadef, 2003). Raindsplash (Ellison, 1944, 1947; Fox and Rorke, 1999) is a significant hillslope degradation agent. Especially in less cohesive, permeable soils, active splash degradation contributes to slope erosion (B., 1985). Few studies have taken into account a range of slope angles and natural rainfall conditions (Fox and Rorke, 1999; Van Dijk et al., 2003b,a). On steeper slopes splash results in a significant net downslope splash transport of soil particles, as confirmed both in the lab and in the field under controlled conditions of simulated rainfall (De Ploey and Savat, 1968; Mosley, 1973; Torri and Poesen, 1992; Kirkby, 1988; Poesen and Savat, 1981; Van Dijk

et al., 2003a; Pietraville et al., 2001).

Rain causes four major effects on a hillslope: dissaggregation of soil units as a result of impact, soil creep and lateral displacement of soil particles, saltation of soil particles into the air, and sorting of particles(Poesen, 1986). The last is the result of forcing-fine grained material into soil voids, hence reducing the soil's permeability, and of selective splashing of detached particles. Raindrop impact has been observed to cause compaction of the topsoil, causing surface sealing and crusting (Poesen, 1986; Proffit and Rose, 1991; Wainwright et al., 1995). In general, more water drops and soil particles are splashed downslope than upslope. Experimental results have indicated greatest detachment at angles between 10°and 20°(Froehlich et al., 1986). The curvilinear relationship between slope angle and detachment is influenced by particle size and at low angles, grains are splashed upslope and downslope at an equal rate, resulting in a net downslope transport of particles close to zero(De Ploey and Savat, 1968). Erpul and Gabriels (2003) observed wind to be a critical factor influencing splash, as it increases the raindrop's kinetic energy and affects the impacting angle, therefore influencing the impact energy. Poesen (1985); Savat and Poesen (1981); Erpul and Gabriels (2003) indicate that surfaces with very fine to fine sand are most susceptible to detachment by raindrop splash, as well as to turbulent run-off, wind, and sheet and rill erosion. Intensity and size of raindrop impact are also important factors that control particle transport due to splashing (Ellison, 1947).From Laws (1941); Laws and Parsons (1943); Ellison (1947) our rainfall intensities can be classified as torrential (93mm/h) heavy rain (2mm/h) and mist to drizzle (0.08 mm/h) from rain intensity measurements.

The above studies summarize the particle detachment dependence of kinetic

energy and diameter of drop, median grain size of material and surface cover and slope gradient. All these studies have gathered a database of rainsplash measurements, yet it is uneven, mostly due to the problem of short duration of the period of investigation, and unpredictable weather.These data are in need of calibration and benchmarking against measurements taken under natural conditions, as pointed out by many authors, e.g. Silva et al. (1998); Van Dijk et al. (2003a).

The goal of this study is to inquire whether it is possible to collect data on raindrop impact erosion on natural hillslope under natural conditions with varying surface cover and slope gradients to allow benchmarking of experimental data and models. We examine whether the erosion pattern of a less cohesive permeable loam sand soil follows the previously observed relationship between event-scale rainfall and erosion of cohesion, loess type soil (Ellison, 1944; Schultz et al., 1985; Wainwright et al., 1995; Mermut et al., 1997; Mouzai and Bouhadef, 2003). We make observations of exponentially increasing splash erosion till ponding is achieved, on a range of slopes between 0°and 30°but that at the same time the first storm of the season moves most sediment, even though it may rain as much within the season again, without moving as much sediment.

The present work explores measurements of 23 rainsplash sample sites using splashboard instruments (Ellison, 1944). The raindrop impact data were collected in the northwestern San Francisco Volcanic Field, Arizona (AZ), over a course of five years during five monsoonal seasons on the hillslopes of two weathered scoria cones. We present raw data with implications, interpretations, and comparisons to previous work.

Measurements focus on rainfall amount and the downslope and upslope splashed mass moved at different sites along hillslopes. Two scoria cones were chosen for this study due to the advantages of their simple initial geometric shape, size, homogeneous particle composition and weathering stage.The vegetation on one of these cone was destroyed by a wildland fire before collection of any samples, allowing for some insight into rainsplash erosion after forest fire (Fig.1).

2 Location

The location chosen for this study is the San Francisco Volcanic Field, AZ, a Neogene scoria cone field consiting of Miocene to Holocene volcanic rocks overlaying Tertiary sedimentary rock of the Colorado Plateau. The scoria cone field is spread over an area of 1800 sqmiles and includes over 600 vents. The age of the vents decreases from west to east. Due to the great difference in age the cones show different stages of erosion and maturity.

Two scoria cones, Wild Bill Hill (111°, 50′50″W, 35°19′30″N) and Walker Lake Crater (111 °, 44′0″W, 35 °, 23′30″N), composed of loose basaltic scoria (Wolfe et al., 1987), were the main focus for the collection of hillslope degradation data due to active rainsplash erosion under natural conditions of climate and slope cover (Fig. 2). The area's climate is seasonal and monsoonal storms during the summer months allow event scale observation and collection of data due to the active degradation. Wild Bill Hill, located west of San francisco Peak, is 0.35 m. y. (Wolfe et al., 1987) and of the later Planeze stage (Kear, 1957). Its foot lies at 2580 m while its highest point lies at 2730 m. The cone is dissected by four main channels, two of which show intensive erosion and little to no

vegetation in the upper reaches, bearing material unprotected to weathering.

Walker Lake Crater located NNW of San Francisco Peak, is 2.01 ± 0.22 m y old (Wolfe et al., 1987), and in the Late Volcano, early Planeze stage (Kear, 1957). Walker Lake reaches from 2660 m to 2837 m. A crater is observable and contains water forming a small crater lake (Fig. 3). This volcano is believed to be of phreatomagmatic nature since the crater width is consistent with a tuff ring (Blauvelt, 1998). The volcano is 5 km away from Saddle Mountain, which erupted approximately 15440 years ago (ref abstract 2004 GSa rocky mountain meeting) and left the southwestern/western side of Walker Lake crater blanketed with fresh, unconsolidated uncohesieve basaltic scoria. The thickness of the deposit is estimated to be between 1 m and 2 m. This scoria is easily eroded and has a much higher infiltration rate than the older underlying basaltic regolith. Two fires in 1996 destroyed large parts of this volcano's vegetation cover, leaving bare surface in many areas behind. Areas of high, medium,and low to no fire severity were distinguished for rainsplash measurements.

The vegetation of both sites varies from dense Ponderosa Pine and Quaking Aspen forest (*Pinus ponderosa and Populus tremuloides*) to grass-covered (*Bushgrasses*), and barren slopes from 1.7°to 29.5°. The composition of both cones is slightly weathered basaltic regolith, implying that the main force of erosion is physical weathering (Peltier, 1950).

3 Climate

The SFVF is located in a region of semiarid climate. At an average elevation of 2150 m among the cinder cones west of the peaks, the temperature rarely rises above 32°C, and for most of the summer the mercury lies around 29°C. In winter, the coldest microclimates in the SFVF area may plunge to -28°C, with lows between -17°C and -12°C being typical in the lower elevations of the volcanic field. Between December and March, a southward shift of the jet stream normally brings up to 2500 mm of snow to Flagstaff, the biggest town within this region. A similar long-term shift of an Atlantic high into the Gulf of Mexico brings a monsoonal flow of moisture during July and August. This 'monsoon' brings the area an average of 127 mm of rain over the whole summer, with average annual precipitation around 630 mm. These summer rainfalls occur in the form of strong, heavily loaded, local thunderstorms, causing such features as overland flow in the form of flash floods and debris flows. Precipitation is recorded for the winter period in the form of snowfall. The summer precipitation though is considered most effective on hillslope evolution because of its intensity at event time. Peltier (1950) hypothesized with climate process diagrams that mechanical weathering was the main weathering feature in semiarid environments and only little chemical weathering took place. This suggests also that mechanical degradation at the time of intense rainfall events is most likely to occur and to be the main degradation feature.

As a rainstorm event begins, the usually dry soil surface experiences mechanical raindrop and hail impact, splashing sediment particles in all directions into the air and moving them from their original location (e.g. Torri and Poesen (1992)). The rain characteristics in the San Francisco Volcanic Field monsoon

season can be classified as a torrential (93mm/h), heavy rain (2mm/h), or mist to drizzle (0.08 mm/h), comparing rain intensity measurements we have made to literature (Laws, 1941; Laws and Parsons, 1943; Ellison, 1947).

4 Methods

4.1 Instruments

Many laboratory studies measured splash erosion using splashcups (Torri and Poesen, 1992; Mouzai and Bouhadef, 2003). In contrast, the splashboard instruments used to conduct this investigation are designed after the idea of Ellison (Ellison, 1944). The splashboards consist of two 50 cm long troughs that are 10 cm wide and 5 cm deep. The troughs are glued together along their long axis and divided by a Plexiglas area of 50 cm by 50 cm, which is securedto the troughs by a small tongue, to avoid trickling of the upslope splashed sediment into the downslope splashed sediment trough and vice versa. The tongue is 1 cm wide, forming a half circle, and is attached permanently to the Plexiglas board (Fig. 4). Two small holes in each side of the board are used to wire it to two $100cm$ long iron stakes, which are secured in the ground, so the board is not blown over by the wind. These stakes are set into the ground parallel to the gravity vector and tangent to a countour line. The construction is therefore set up with the long axis of the troughs tangential to a contour line of the slope and with the Plexiglas area parallel to the gravity vector. The troughs have been dug into the soil surface as carefully as possible and stand 1.5 to 2 cm above the ground surface in both downslope and upslope facing directions.

The set-up allows splash going upslope to fall into the downslope facing trough or to cohere to the downslope facing board. Downslope-going splash is caught on the upslope facing trough and board. This enables determination of the net downslope flux of sediment.By direct observation, splash at the study sites seldom exceeds 50 cm height in saltation, enabling most of the splash to be caught by the trough, after trickling down the board (Fig. 4). It has been unusual to move the boards in the literature, but moving of boards after two seasons of intense rainfall activity to a naturally intact, similar, nearby location on the slope is essential due to wash-out of particles (Fig.5). Consequently, if the season was dry the boards need not be moved.

4.2 Data collection

Immediate presence in the field is essential to obtain a good rainsplash sample, so that measurements of the rainfall amount and possibly the rainfall duration, and the collection of the rainsplash sample occur directly after a rainfall event and an overlap of events can be ruled out. After each event, samples are collected by brushing the particles stuck on the board into the trough, then carefully removing the board and the trough from its location. This needs to happen with minor impact to the surface, a mold will be left in the ground, into which the troughs will be replaced. Both troughs need to be permanently marked 'upslope facing' or 'downslope facing' to avoid sample confusion, as the troughs are removed for sample collection. With the help of degradable filter or toilet paper (for a wet sample), a brush (for a dry sample) and a scraper, the sample is removed from the trough and placed in a plastic sample bag. The first sample from each instrument was discarded, to allow the slightly

disturbed surface regain its natural status. In the laboratory, the samples are treated after Goudie (Goudie, 1981); they are dryed, organics removed, weighed, and sieved. Unlike the splashcups used by, e.g., Torri and Poesen (Torri and Poesen, 1988), we obtain separate measurements for upslope and downslope transported sediment. It proved difficult to be at the individual sites at the exact onset and finish of rainstorms, since they are quite local and short-lived. As expected, upslope splash sediment yield forms a smaller sample and is prone to larger error.

Data were collected from 1996 to 2000 on varying slope gradients and under different slope cover conditions ranging form grassy to barren and different stages of burn severity (Fig. 6).

5 Analysis

We first calculate actual netdownslope sediment fluxes with help of previous author's works. This is followed by a statistical analysis of the dataset involving wildland fire, to see if there is an imapct of the varying fire severities on the netdownslope flux.

Several authors have investigated the influence of slope angle on the downslope and uplsope splashed fraction of a rainsplash sample (Ellison, 1944; Ekern and Muckenhirn, 1947; Ploey, 1969; Mosley, 1973; Rosewell and Martson, 1978; McCarthy, 1980; Kerenyi, 1981; Poesen and Savat, 1981). The relationship between slope angle and rainsplashed sediment is well represented by the following equation (Poesen, 1985):

$$\frac{M}{M+m} = 0.50e^{-b\alpha} \tag{1}$$

where M is the downslope splashed sediment of a splashboard, m is the upslope splashed sediment of a splashboard, $M/M+m$ is the downslope splashed fraction of the sample, α is the local slope angle, and b is a coefficient. We calculate b-values for individual spalshboards to compare to b-values from previous authors.

To be able to convert our collected sediment masses to a netdownslope sediment flux, an estimate of the mean splash distance of the splashed particles is needed. Mean splash distances are perpendicular to the countour line and can be obtained by using

$$y_{downslope} = 0.019(D_{50})^{-0.22} + 0.301 \sin \alpha \tag{2}$$

and

$$y_{upslope} = 0.019(D_{50})^{-0.22} - 0.301 \sin \alpha \tag{3}$$

respectivley (Poesen and Savat, 1981), where D_{50} is the mean grainsize of the splashed sediment sample and $y_{downslope} and y_{upslope}$ are the mean splash distances. The conditions for the latter equation are mean grainsizes of $0.02mm \leq D_{50} \leq 0.7mm$. For our purposes, we have extrapolated the lower limit to $0.01mm$. Careful consideration was given to determine the affected length of slope through which the flux was going. Only the downslope splash distance is needed to finally determine the netdownslope sediment flux and the lenth of the splashboard ($0.5m$) to obtain a flux in the form of $m^3 m^{-2} a^{-1}$.

To find erosion rates in the form of volume per sqm per precipitation event,

we used the general mass conservation equation

$$\frac{F_{netdownslope}}{\delta y_{downslope}} = \frac{\delta h}{\delta t} \tag{4}$$

This can be expressed as

$$\frac{\delta h}{\delta t} = \frac{\frac{M-m}{y_{downslope} l_{sb} \rho_{bulk}}}{\delta t} \tag{5}$$

where $\frac{\delta h}{\delta t}$ is the change in height per event expressed in volume per square meter per precipitation event,$M - m$ the net downslope mass of the splashed particles of one sample, ρ_{bulk} the bulk density of the area surrounding the splashboard, $y_{downslope}$ the mean downslope splash distance, and l_{sb} the length of the catching board along the countour, in our case consistently $0.5m$, and δt is time between individual events.

To be able to compare our results to other authors and retrieve erosion rates in a form of volume per square meter per year, all the data collected in one year were summend up to represent the material moved in one season. Since we have an average of five seasons-worth of data, the five years are analysed both, individually, and together. Therefore the previous equation becomes:

$$\frac{F_{indv.year,netdownslope}}{\delta t} = \left(\sum_{i=1}^{n} \frac{M_i - m_i}{y_{downslope} l_{sb} \rho_{bulk}} \right) \left(\frac{1}{1 \text{ yr}} \right) \tag{6}$$

and the data is then averaged for each individual splashboard over the course of the five seasons.

Since we had 23 splashboards, we obtain 23 netdownslope sediment yields that represent the change in height of the regolith's surface per sqm per year averaged over five years due to raindrop impact.

For the statistical analysis, ANOVA and multiple regression were used. A standard anova package (www.statsoft.com, 2006) was used, while the multiple regression is based on the general form of the following equation ((Davis, 1986)):

$$Y_{general} = \beta_0 + \beta_1 S + \beta_2 V + \beta_3 F + \beta_4 P \tag{7}$$

Where S is slope gradient [deg], V is vegetation cover %, F is fire severity $[3 = High, 2 = Medium, 1 = Low]$, P is precipitation $[cm]$, and β_i are the regression coefficients. The latter were obtained by writing our own matrix in an spreadsheet after Davis (Davis, 1986).

The results from the applied multiple regression are a means to find a linear model that best describes the data with multiple independent variables, to see which variable is most significant by comparing the standarized coefficients to one another. As is nature of the multiple regression, it is needed to standarize the coefficients to be able to compare the relationship between the different β values (Davis, 1986).

Vegetation cover at each site was determined by counting vegetation within a set grid for all locations, simmilar to that of determinig percentage of black minerals in a rocksample.

Fire severity was determined by the Rocky Mountain Research Station technique. If only some grasses and the lower tree trunks are scorched, the fire severity is considered low. If the tree trunks are scorched in the lower trunk to mid-height, most pine needles are brown, eventually falling off to cover the ground surface, and only the crown remains with some green needles, the fire severity is considered medium. Both low and medium fire severity damage is

considered part of the natural ponderosa-aspen-fire cycle. The tree and vegetation around the tree will fully recover. High severity fire damage is considered unnatural. In this case, the trunk is severed to death by very high temperature fire and the duff containing seeds that usualy germninate with low or medium fire severity temperatures, are completly destroyed. Only the main trunk with a few thicker branches is left standing as charchoaled remnant of the healthy tree.

6 Results

The data shown in this study are representative of 337 individual down and upslope splashed sediment measurements. Net downslope sediment weight was determined by subtracting the upslope splashed part of a sample from the downslope splashed part. Figure 13 summarizes the sum of the individual splashed net downslope sediment next to the precipitation. After sieving about half the population to obtain mean grainsizes, the remaining D_{50} are calculated by taking the average of the sieving results for each individual site. Equations (2, 3) are used to calculate splash distances (Fig. 11, Fig. 12). After the mean splash distances are determined, Equation (5) is used to obtain the individual $F_{ind.year,netdownslope}$ per rainfall event, where a total of 152 pairs of $M - m$ are used. The data are averaged over the 5 years they were collected. We obtain an average yearly net downslope sediment flux with equation (6), and plot against the average yearly rainfall amount that caused the splash for each individual site (Fig. 14). This data shows the change in height of the soil surface per year and the amount of rainfall involved.

After determining the net downslope flux of the splashed sediment, the sed-

iment splash follows a general trend of exponential increase as slope angle increases, which also depends on precipitation amount and vegetation cover (Fig.6).

The data indicate consistent exponential erosional behavior due to raindrop impact before the ponding threshold is reached on slopes between 1 °and 30 °when analysed in an individually and on event-scale. With increasing slope gradient the amount of soil particles moved out of unit area increases and varies by orders of magnitude. Fig.6 shows the downslope splashed part of the individual sample sites. An exponential curve fit is applied to the data below the ponding threshold. The downslope splash correlation resulted in a best fit for some individual splashboard sites of $R^2 = 0.98$ and an average of $R^2 = 0.37$ for all splashboards (Fig. 6, Table 1). The upslope splash correlation resulted in a best fit of $R^2 = 0.97$ for some individual splashboard sites and an avarage of $R^2 = 0.48$ for all splashboards. Both fits are satisfactory taking into account that rainsplash is shown against rainfall amount rather than rainfall intensity. When using all data to plot the ratio between downslope sediment and the sum of the downslope and upslope splashed sediment against slope angle, it compares to previously summarized data that included experimental and splash cup rainsplash measurements (Fig.7) (Poesen, 1985). Our b values for a curve fit (Equation 1) are $b = 0.0479$. Previous author's b-values for field data lie between $0.035 \leq 0.089$ for fine sand to coarse sand. our data is a mix of different ratios of clay size particles to coarse sand size particles.

In general our raw data indicates a threshold behavior at $2.5 - 3.0cm$ rainfall (equivalent to $1.25mmh^{-1}$ rainfall intensity) (Fig. 8). We observe an exponential increase of sediment yield during rainstorms before ponding is reached for all of our sample sites, regardless of vegetation cover and location on hills-

lope. Once saturation sets in during the season, and overland flow begins, the erosion due to direct rain drop impact decreases dramatically (Fig. 8). The plottet curve in Fig. 8 is a smooting curve, showing the increase to threshold and decrease after ponding is reached. We consider this the threshhold for individual event scale data.

The averaged data (14) does not show a clear threshold behaviour around $2.5cm$ of rainfall as seen in the raw individual data. However, does show a peak of sediment flux at $3.25cm$ even under varied circumstances , such as fire severity, vegetation cover and slope angle. For example, Figure 7 raw data (sediment weight) is shown for rainfall amounts of $2.91cm$, slightly above the $2.5cm$ ponding threshold. Since the data is field data under natural conditions, our data scatters as expected. When comparing our data with previous studies from mostly experimental raindrop impact, it falls nicely within various author's fitted curves (Poesen, 1985).

The first major rainstorm causes much more erosion than do later rainstorms in the same season (Figures 9 and 10). We observe a peak sediment transport in the beginning of the season, while later in the season less intense sediment transport is recorded at similar amounts of rainfall. What causes this phenomenon? From direct field observation, this is caused by increasing moisture-driven cohesion of the regolith and seasonal vegetation growth. At the beginning of the monsoon season, the grasses are dry or non-existent, leaving the surface more prone to erosion. As the rainy season progresses, the vegetation grows and begins to cover the surface with a protective layer. The influence of vegetation cover on raindrop erosion shows that our rainsplash data are in harmony with Jansson's observations (Jansson, 1982) that smaller raindrop sizes cause less net mass movement. We observe in areas of dense

vegetation cover that less material is splashed, because the raindrop energy is buffered by vegetation cover, as vegetation splits raindrops into smaller drops (Calder, 1996).

6.1 Fire damage

After a destructive wildland fire significantly altered the vegetation cover on Walker Lake Crater in 1996(Nijhuis, 1999), we obtained observations relating to regotlith erosivity in direct connection with the fire damage to the vegetation.

To statistically analyse the high, medium, and low to no-fire severity the Analysis of Variance is used. We can say that three distinct (high, medium and low to no-fire severity) groups of erosion behavior can be distinguished that correlate to the fire severity level. The probability that the null hypothesis is correct (there are no fire severity related populations distinguishable from the dataset), that the effect of fire severity is not a significant factor and has no impact on the erosion rate, is $P = 0.03$. For our data this means that the null hypothesis can be rejected at the $\alpha = 0.05$ significance level (Table 3 and Fig. 1). Within the 95% confidence interval, high fire severity areas can be distinguished from the medium and low fire severity locations. The medium to low fire severity populations are also distinguishable, but not as clearly, as can be expected from looking at Fig. 1.

Multiple regression analysis of both the Wild Bill Hill (no fire) and the Walker Lake Crater (fire) individual event data suggests that for a burned, natural hillslope, the remaining vegetation cover is the most important independent

variable to prevent erosion by rainsplash (negative factor in the standarized multiple regression equation). Fire, where present, is the factor that correlates most strongly with erosion, followed by precipitation amount (and rainfall intensity) and slope gradient. Interestingly, for a burned hillslope, the significance of slope gradient is lessened (Table 2). The resulting multiple regression equations (7) are as follows:

$$Splash_{WLC} = 3.11 + 0.12 * (S) + 1.46 * (F) - 0.09 * (V) + 0.99 * (P) \quad (8)$$

Standarized:

$$Splash_{WLC} = 3.11 + 0.08 * (S) + 0.18 * (F) - 0.32 * (V) + 0.15 * (P) \quad (9)$$

and

$$Splash_{WBH} = -9.32 + 1.42 * (S) - 0.16 * (V) + 5.21 * (P) \quad (10)$$

Standarized:

$$Splash_{WBH} = -9.32 + 0.21 * (S) - 0.12 * (V) + 0.16 * (P) \quad (11)$$

For the multiple regression $R^2 = 0.3$. The data are collected under natural conditions. The R^2 projects a multidimensional non-linear problem into a two-dimensional linear representation and includes all data from the individual splashboards on the burned and the unburned scoria cones under varying rainfall conditions, seasonal vegetation growth and annual variance of precipitation conditions. The multiple regression indicates that a major wildland fire with high severity (Table 2) has tremendous impact on the rain-splash erosion behavior, making areas of fire damage with less vegetation significantly more

prone to erosion by rainsplash. On the other hand, on an unburned cone, where healthy, intact vegetation cover is evenly spread, slope gradient and precipitation seem are more important to rainsplash erosion than vegetation cover.

Directly after the wildfire, areas of medium, high and low severity were distinguished in the field. A big storms at the beginning of the season move more particles than at the end of the rainy season (Fig. 9). The behavior of erosivity in the medium to low fire severity damaged areas is intriguing: The protection from raindrop impact that the vegetation offers to the soil surface is of particular importance to areas on the hillslope with medium fire severity damage, where fallen dry pine needles covered the scorched soil surface shortly after the fire dissipated. Immediately after the fire a rain storm of $58.6 mm/h$ rainfall intensity occured, lasting 30 minutes, depleting the barren hillslopes of loose particles in enormous quantities, and generating numerous small debris flows, before the protecting pine needles have a chance to fall onto the surface. The areas depleted of vegetation due to high fire severity, show strongly increased sediment movement, likely eroding as previously barren areas. Areas of medium to low severity burn, showed an effect of the fallen brown pine needles as a protective cover. However, erosion is simmilar to those of barren areas before the pine needles cover the ground. Once the areas is coverd with pine needles they were treated as if covered by a high percentage of vegetation. We observe, at pine needle covered surfaces, that mass transport by rainsplash is minor, but still shows the observed threshold behavior (Fig. 1).

6.2 Erosion Rates

The values for the obtained for splashdistances and netdownslope sediment fluxesare within the orders of magnitude from experimental data. For example, Poesen's experimental fluxes are $F_{poesen} = 0.0180 m^3 m^{-2} a^{-1}$ for dune sand with a $D_{50} = 0.230 mm$, dune slope angle $\alpha = 30\ ^\circ$, and a kinetic energy of rainfall $K.E. = 9937 J m^{-2} a^1$. Our values lie between $10^{-5} \leq F_{martinez} \leq 10^{-3} [m^3 m^{-2} a^{-1}]$ for $0.01 mm \leq D_{50} \leq 0.7 mm$, slope angles between $1.7^\circ \leq \alpha \leq 29.5^\circ$, for scoria cones ages $0.3 ma$ to $2.01 ma$ with varying regolith cohesion, precipitation events of $0.1 cm \leq precipitation \leq 6.1 cm$, vegetation cover from 0% to 100% , and with wildland fire impacted sites (high, medium, low and no fire severity).

7 Conclusions

Five years of rainsplash data collection under natural rainfall conditions are presented in this study. Although scatter is seen in the data set, we are able make the following observations: event scale data show threshold behavior around $2.5 cm$ of rainfall regardless of vegetation cover, slope angle, or soil bulk density. During storms, more particles are disaggregated increasing loose particle availability, mobility while mass transport increases seemingly exponentially until a ponding threshold is reached. The beginning of the rainy season causes most of the sediment yield due to raindrop impact. Rainfall in the later season does not cause as much sediment yield. High fire severity is a distinguishable statistical parameter and results in a statistically significant increase of sediment yield in orders of a few magnitudes.

Acknowledgements

This research was supported by grant by NASA NAG53142 to study landscape evolution. We thank the Flagstaff United States Forest Service for permissions to work and set up instrumentation in the Coconino National Forest.

References

Bauer, B., 1985. Contribution of splash to soil erosion by water. In Soil Conservation and Productivity. IV International Conference on Soil Conservation. Pla Sentis, I.(ed.), Maracay-Venezuela (pp. 82-93).

Blauvelt, D. J., 1998. Examples of scoria cone degradation in the San Francisco volcanic field, Arizona. SUNY at Buffalo, Amherst, NY, United States.

Calder, I., 1996. Dependence of rainfall interception on drop size; 1, development of the two-layer stochastic model. Journal of Hydrology 1-4 (185), 363–378.

Davis, J. C., 1986. Statistics and data analysis in geology, 2nd Edition. John Wiley and Sons, Inc.

De Ploey, J., Savat, J., 1968. Contribution a l'etude de l'erosion par le splash. Z. fur Geomorphologie 12, 174–193.

Ekern, P., Muckenhirn, R., 1947. Water drop impact as a force in transporting sand. Soil Sciences Society Am. Proc. 12, 441–444.

Ellison, W., 1947. Soil erosion studies. Agricultural Engineering 28, 145–146.

Ellison, W. D., 1944. Studies of raindrop erosion. Agricultural Engineering 25, 131–136, 181–182.

Erpul, G.and Norton, L., Gabriels, D., 2003. Splash saltation trajectories of soil particles under wind-driven rain. Geomorphology.

Fox, D., Rorke, B., 1999. The relationship of soil loss by interril erosion to slope gradient. Catena 38, 211–222.

Froehlich, W., Vogt, H., Slaymaker, O., 1986. Influence of the slope gradient and supply area on splash scope of the problem. Zeitschrift fuer Geomorphologie, Supplement 60, 105–114.

Goudie, A., 1981. Geomorphological techniques. London; Boston: Allen and Unwin.

Jansson, M., 1982. Land erosion by water in different climates. Ph.D. thesis, Uppsala University, Dep. Phys. Geogr., Sweden, uNGI Rapport (57), Uppsala Univ. Doctoral thesis; CNRS-18566.

Kear, D., 1957. Erosional stages of volcanic cones as indicators of age. New Zealand Journal of Geology and Geophysics.

Kerenyi, A., 1981. A study of the dynamicsof drop erosion under laboratory conditions. Publ.IAHS 133, 365–372.

Kirkby, M., 1988. Hillslope runoff processes and models. Journal of Hydrology 100 (1-4), 315–319.

Laws, J., 1941. Measurement of fall-velocity of water drops and raindrops. In: Measurements of fall velocity of water drops and raindrops. Vol. 22. Trans. Am. Geophysical Union, pp. 709–721.

Laws, O., Parsons, A., 1943. The relation of raindrop size to intensity. Trans. Am. Geophysical Union.

McCarthy, C., 1980. Sediment transport by rainsplash. Ph.D. thesis, University of Washington, Seattle.

Mermut, A. R., Luk, S. H., Roemkens, M. J. M., Poesen, J. W. A., 1997. Soil loss by splash and wash during rainfall from two loess soils. Geoderma 75 (3-4), 203–214.

Mosley, M., 1973. Rainspalsh and the convexity of badland divides. Zeitschrift

f́ur Geomorphologie, Suppl. 18, 10–25.

Mouzai, L., Bouhadef, M., 2003. Water drop erosivity: effects on soil splash. Journal of Hydraulic Research 41 (1), 61–68.

Nijhuis, M., March 1st 1999. Flagstaff searches for its forest's future. High County News, vol.31 No. 4.

Peltier, L., 1950. The geographic cycle in periglacial regions as it is related to climatic geomorphology. Annals of the Association of American Geographers 40, 214–236.

Pietraville, S., van den Bosch, F., Welham, S., Parker, S., Lovell, D., 2001. Modelling of rainsplash trajectories and prediction of rain spalsh height. Agricultural and Forest Meteorology, 171–185.

Ploey, D., 1969. L'érosion pluviale: expériences à l'aide de sables traceurs et bilans morphogénique. Acta Geographica Lovaniensa 7, 1–28.

Poesen, J., 1985. An improved splash transport model. Zeitschrift fuer Geomorphologie 29 (2), 193–211.

Poesen, J., 1986. Surface sealing as influenced by slope angle and position of simulated stones in the top layer of loose sediments. Earth Surface Processes and Landforms 11 (1), 1–10.

Poesen, J., Savat, J., 1981. Detachment and transportation of loose sediments by raindrop splash; II, Detachibility and transportability measurements. Catena (Giessen) 8 (1), 19–41.

Proffit, A., Rose, C., 1991. Soil erosion processes; i, the relative importance of rainfall detachment and runoff entrainment. Australian Journal of Soil research 29 (5), 671–683.

Rosewell, C., Martson, D., 1978. The erosion process as it occurs within cropping systems. Journal of Soil Conservation Services, New South Wales 34,

186–193.

Salles, C., Poesen, J., 2000. Rain properties controlling soil splash detachment. Hydrological Processes 14 (2), 271–282.

Savat, J., Poesen, J., 1981. Detachment and transportation of loose sediments by raindrop splash; I, The calculation of absolute data on detachability and transportability. Catena (Giessen) 8 (1), 1–17.

Schultz, J., Jarrett, A., Hoover, J., 1985. Detachment of splash of a cohesive soil by rainfall. Am. Soc. of Agricultural Engineers, 1878–1884.

Silva, R., Ferreira, A., Tomas, P., 1998. Rainfall characteristics and soil erosion in alentejo. Geoekodynamik.

Torri, D., Poesen, J., 1988. Incipient motion conditions for single rock fragments in simulated rill flow. Earth Surface Processes and Landforms 13 (3), 225–237.

Torri, D., Poesen, J., 1992. The effect of soil surface slope on raindrop detachment. Catena (Giessen) 19 (6), 561–578.

Van Dijk, A., bruijnzeel, L., Eisma, E., 2003a. A methodology to study rain-splash and wash processes under natural rainfall. Hydrological Processes.

Van Dijk, A., Bruijnzeel, l., Wiegman, S., 2003b. Measurements of rain spalsh on bench terraces in a humid tropial steepland environment. hydrological Processes 17, 513–535.

Wainwright, J., Parsons, A. J., Abrahams, A. D., 1995. A simulation study of the role of raindrop erosion in the formation of desert pavements. Earth Surface Processes and Landforms 20 (3), 277–291.

Wainwright, J., Parsons, A. J., Abrahams, A. D., 1999. Field and computer simulation experiments on the formation of desert pavement. Earth Surface Processes and Landforms 24 (11), 1025–1037.

Wolfe, E. W., Ulrich, G. E., Newhall, C. G., 1987. Geologic map of the north-

west part of the San Francisco volcanic field, north-central Arizona. Miscellaneous Field Studies Map - U. S. Geological Survey, (2 sheets).

8 Tables

Table 1

Exponential fit equations for the upslope splashed sediment at individual sites and for the downslope splashed sediment at individual sites.

Splashboard	*Slope angle [°]*	*Vegetation cover*	*Exponential fit EQ*	R^2*value*
sb 17	21	barren	$y = 0.55 * e^{1.65x}$	0.98
sb 5	11.2	barren	$y = 2.35 * e^{1.21x}$	0.67
sb 4	1.7	some grass and pine needles	$y = 0.52 * e^{1.05x}$	0.90
sb 16	19.5	dense grass	$y = 0.32 * e^{0.66x}$	0.82

Table 2

Standarized and non standarized multiple regression coefficients

Location	*Slope angle coeff*	*Fire coeff*	*Vegetation coeff*	*Rainfall coeff*
WLC	0.12	1.46	-0.09	0.99
WLC stand.	*0.18*	*0.18*	*-0.32*	*0.15*
WBH	1.42		-0.16	5.21
WBH stand.	*0.21*		*-0.12*	*0.16*

Table 3

Analysis of Variance statistics for the fire severity related sites

Fire Severity	*Mean*	*95 p.c. Confidence Int.*	*Standard Dev.*	*Median*
high n=9	6.4	3.36 through 9.43	7.27	3.26
medium n=9	1.06	-1.98 through 4.1	1.26	0.51
low to no fire	1.35	-1.88 through 4.57	1.29	0.76

9 Figures

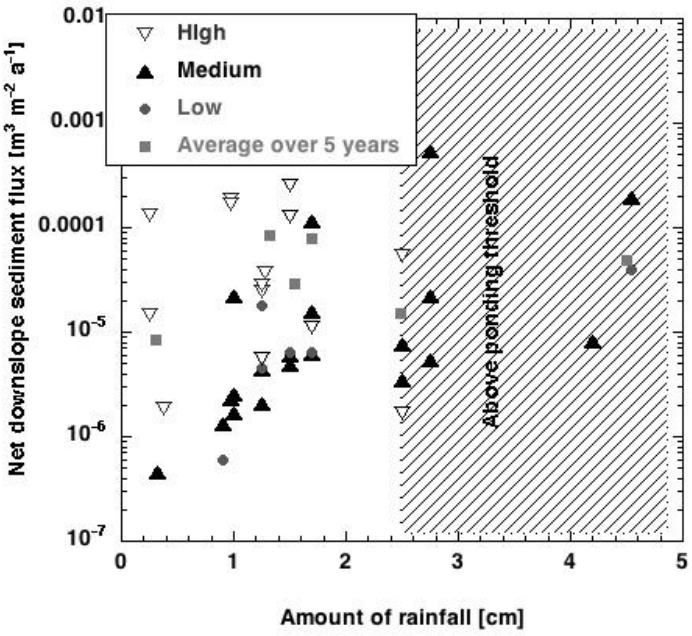

Fig. 1. Increased sediment movement in high severity burned areas of hillslope in dependance of rainfall.

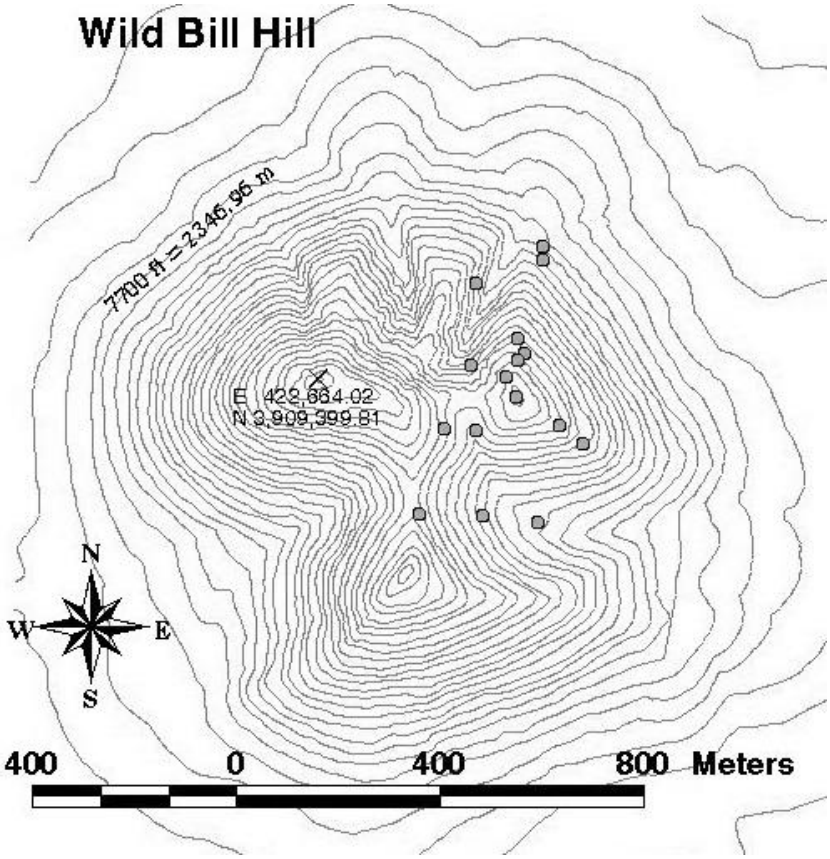

Fig. 2. Splashboard distribution (round dots) on Wild Bill Hill scoria cone, contour interval is 20 ft (6.1 m).

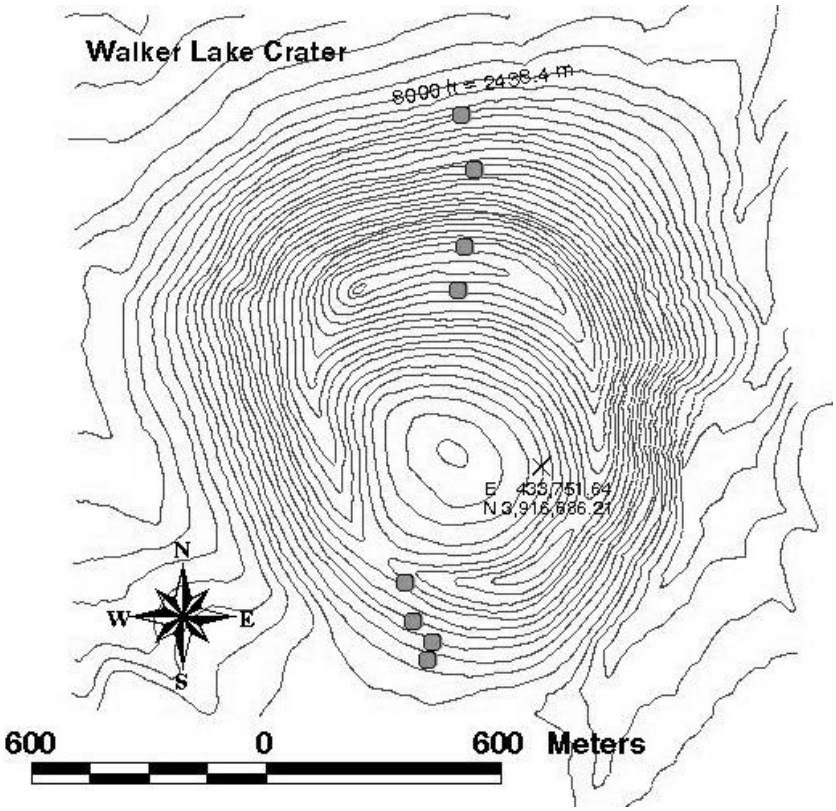

Fig. 3. Splashboard distribution (round dots) on Walker Lake Crater scoria cone, contour interval is 20 ft (6.1 m).

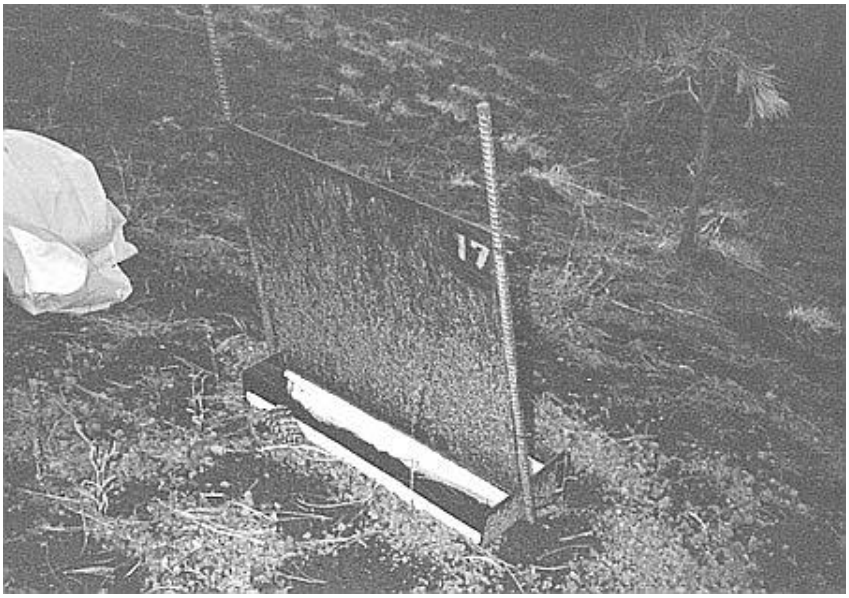

Fig. 4. A splashboard instrument collecting upslope and downslope rainsplashed sediment.

Fig. 5. Particles and soil surface are washed out around the splashboard.

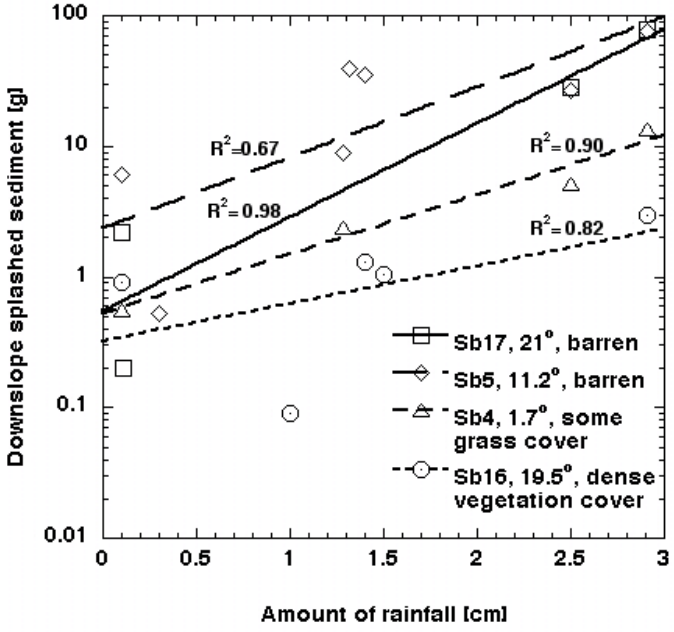

Fig. 6. Examples of exponential behavior of downslope splash with varying vegetation cover and slope angles.

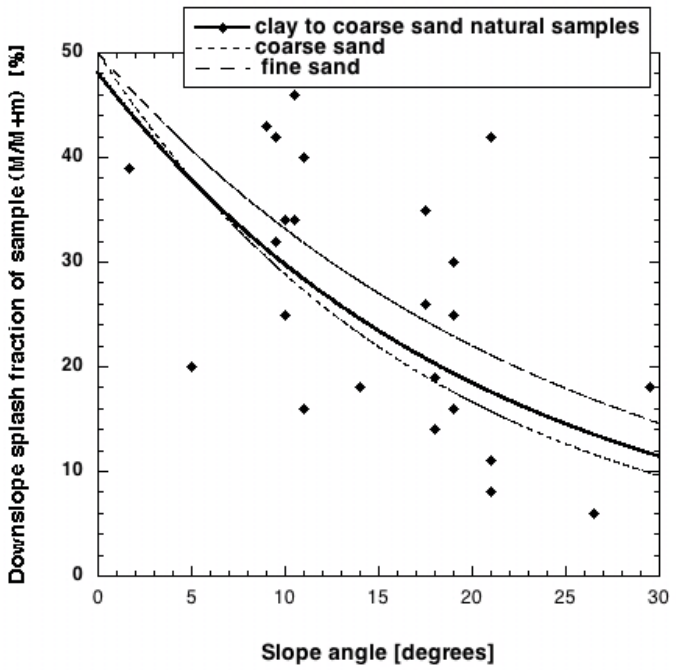

Fig. 7. Relation of downslope splashed fraction (M/M+m) of the total sediment yield detached by raindrop impact. The data is a set of detached sediment following a 2 cm to 2.91 cm rainfall event. Dashed lines represent Poesen's experimental and various other author's summerized laboratory data (Fig. 2 and 3 in 1985 paper (Poesen, 1985)).

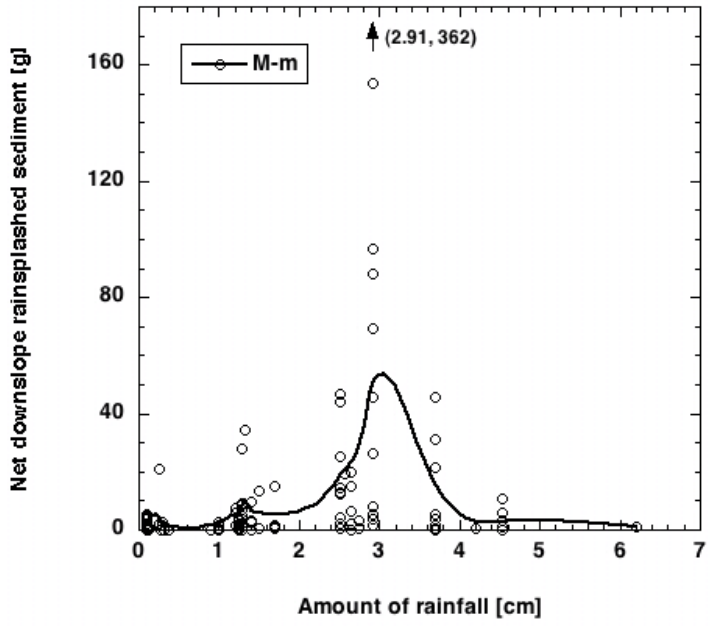

Fig. 8. Net downslope splashed sediment plottet against rainfall amount of all splash-boards for five consecutive rainy seasons (1996-2000). Line is a smoothed curve through the sediment data.

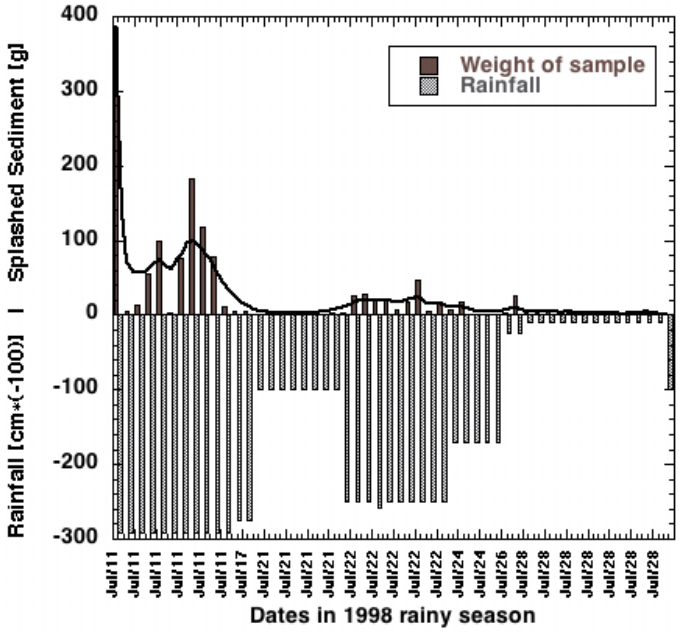

Fig. 9. Downslope splashed sediment in chronological order displaying the correspondant rainfall amount for the 1998 rainy season.

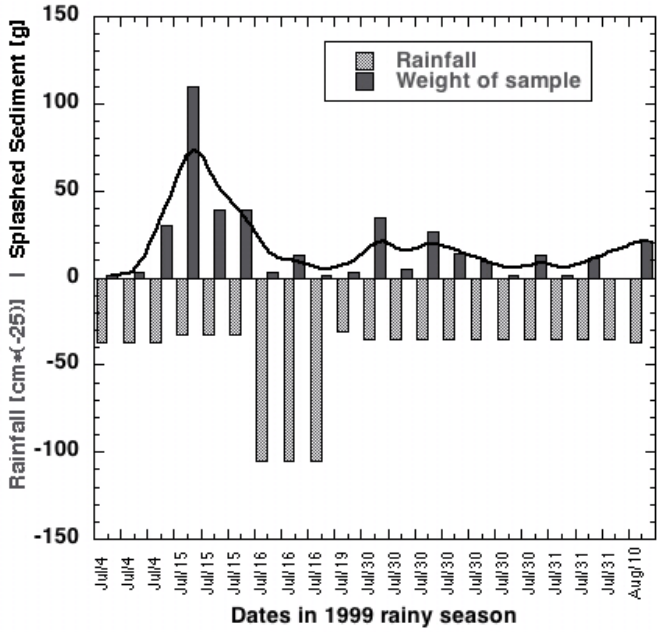

Fig. 10. Downslope splashed sediment in chronological order displaying the correspondant rainfall amount for the 1999 rainy season.

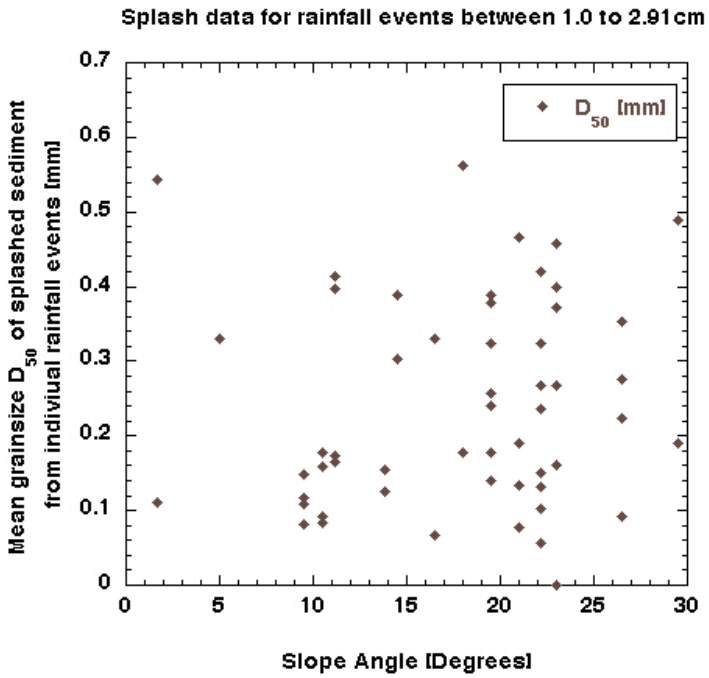

Fig. 11. Individual rainfall events produced splashed sediment within 0.02 to 0.56 mm mean grain size diameter.

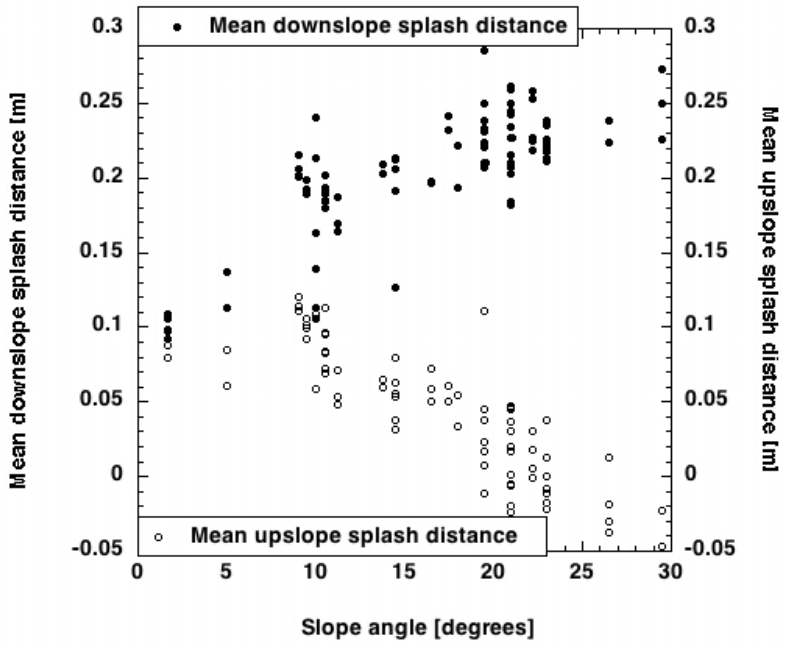

Fig. 12. Individual upslope and downslope splash distances of samples.

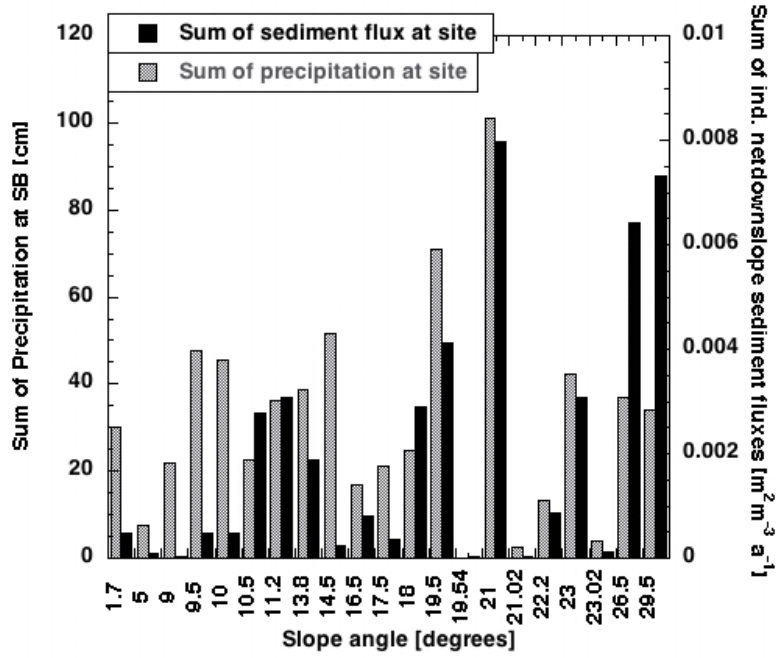

Fig. 13. Sum of precipitation and sum of sediment flux of all individual sites. Higher slope angles depend more on amount of rainfall than smaller angles.

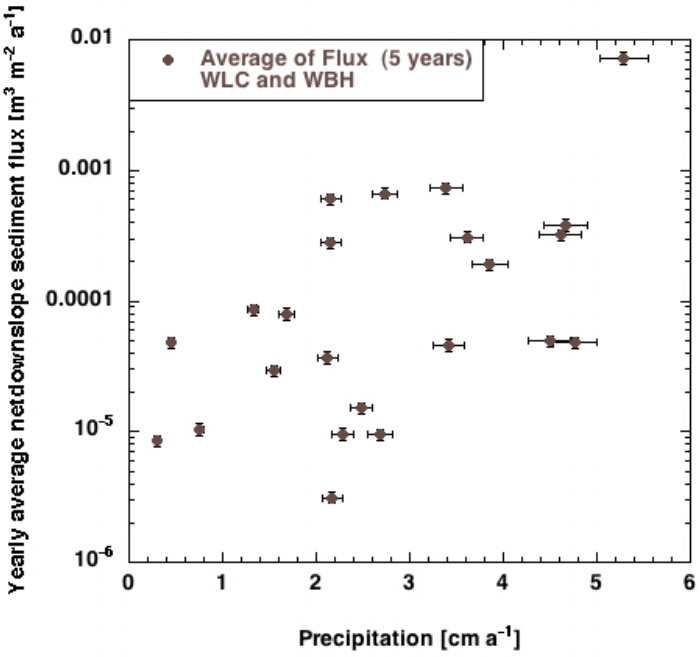

Fig. 14. Yearly average of netdownslope rainsplashed sediment ($n_a = 5$)versus yearly average of measured rainfall at the individual sites.